International Journal of Fatigue 43 (2012) 62–75

Contents lists available at SciVerse ScienceDirect

International Journal of Fatigue

journal homepage: www.elsevier.com/locate/ijfatigue

Correlation of fretting fatigue experimental results using an asymptotic approach

D.A. Hills [a], A. Thaitirarot [a], J.R. Barber [b], D. Dini [c,*]

[a] Department of Engineering Science, University of Oxford, Parks Road, Oxford OX1 3PJ, UK
[b] Department of Mechanical Engineering, University of Michigan, 2350 Hayward Street, Ann Arbor, MI 48109-2125, USA
[c] Department of Mechanical Engineering, Imperial College London, South Kensington Campus, Exhibition Road, London SW7 2AZ, UK

ARTICLE INFO

Article history:
Received 14 September 2011
Received in revised form 3 February 2012
Accepted 7 February 2012
Available online 23 February 2012

Keywords:
Fretting fatigue
Incomplete contacts
Asymptotic methods
Short crack arrest
Frictional energy dissipation

ABSTRACT

Small refinements are made to the bounded asymptotic forms recently developed to encapsulate the state of slip and stress at the edges of incomplete contacts. They are then used to re-analyse several sets of publicly available fretting fatigue data. Several different combinations of the asymptotes are used and it is shown that two are viable and give big improvements upon stress-based criteria. These procedures provide a practical method for both designing against fretting fatigue and quantifying nucleation times when fretting is unavoidable.

1. Introduction

Fretting fatigue is the phenomenon of accelerated nucleation of fatigue cracks by differential slip between contacting surfaces. The first quantitative studies were conducted by O'Connor and co-workers [1–4] with a series of students in the late 1960s and early 1970s. One of the most far-reaching was a set of tests conducted by Bramhall [3], and which appeared only in his D.Phil. thesis, in which very carefully controlled fatigue tests were carried out with cylindrical pads pressed onto the surface, and subject to a shearing force varying harmonically and synchronously with the tension in the specimen. These tests exploit the well-known Cattaneo–Mindlin [5,6] solution for partial slip to give a defined slip regime where the shearing tractions and magnitude of the relative slip displacement are known explicitly at all points. One notable outcome of those tests was a pronounced 'size effect'. It was noted that if a small contact were subject to a particular contact traction regime, and then a second experiment conducted with the *same* tractions and slip, but extending over a larger region, the latter would invariably give a shorter life. These tests were repeated and extended by Nowell [7], who found exactly the same property.

There have been several possible explanations for this effect put forward (see e.g. [8]), but one can argue that none has been demonstrated to be totally convincing. The intention in this paper is not to provide a further candidate, but to describe the environment in which the crack nucleates by an asymptotic form [9–11], and then to display this as a suitable correlator of fatigue life [9,12]. Concepts of threshold stress intensity are well known in plain fatigue and one question which is explicitly addressed here is whether the same, or a modified value, is appropriate for fretting nucleated fatigue. If the threshold for plain and fretting fatigue is the same, this provides evidence that fretting causes no additional damage to the material through the action of rubbing; if the life is reduced then it would follow that there would be no alternative, if threshold conditions were to be found, to carrying out laboratory experiments in the presence of slip.

2. Adhered asymptotes and their calibration

The central idea, here, is to specify the complete local state of stress and slip displacement present at the edge of a contact by two asymptotic forms; one for contact pressure, and one for shear. Only incomplete contacts will be considered and, indeed, we shall restrict ourselves to those which are sufficiently non-conformal for each body to be capable of idealisation by a half-plane. The bodies are also assumed to be elastically similar so that the effects of normal and shear loading are uncoupled; a normal load induces only contact pressure and a shearing force or the application of bulk tension, Fig. 1, induces only shearing tractions. We now 'zoom in' our field of view so that only the very edge of the contact, in the neighbourhood where cracks nucleate, is within view. The local contact pressure, $p(t)$, can then always [9] be written in the form

$$p(t) = K_N\sqrt{t}, \tag{1}$$

* Corresponding author. Tel.: +44 (0)2075947242; fax: +44 (0)2075947023.
E-mail address: d.dini@imperial.ac.uk (D. Dini).

0142-1123/$ - see front matter © 2012 Elsevier Ltd. All rights reserved.
http://dx.doi.org/10.1016/j.ijfatigue.2012.02.006

Nomenclature

a	contact semi-width
a_0	critical length
c	crack depth
C, C'	constants
d	slip zone size
E	Young's modulus
f	coefficient of friction
g_{ij}	eigenfunction related to the spatial distribution of stresses (in asymptotic form) induced by the normal load, with $i,j = x,y,z$
h_{ij}	eigenfunction related to the spatial distribution of stresses (in asymptotic form) induced by the shearing load, with $i,j = x,y,z$
i	complex operator
J_2	second stress deviatoric invariant
k	yield stress in pure shear
K_N	generalised stress intensity factor for the normal traction distribution
$K_T, \Delta K_T$	generalised stress intensity factor and generalised stress intensity factor range for the shear traction distribution
K_T^Q	generalised stress intensity factor for the shear traction distribution due to the application of the shearing force
K_T^σ	generalised stress intensity factor for the shear traction distribution due to the application of the remote bulk tension
$K_I, \Delta K_I$	mode *I* stress intensity factor and stress intensity factor range
$K_{II}, \Delta K_{II}$	mode *II* stress intensity factor and stress intensity factor range
ΔK_{th}	threshold stress intensity factor
$\Delta K_{I,th}$	mode *I* threshold stress intensity factor
$\Delta K_{II,th}$	mode *II* threshold stress intensity factor
p	contact pressure
p_o	peak contact pressure
q	shear traction
Q	shearing force
R	load ratio
$\hat{r}$	r/d – normalised radial coordinate centred at the contact edge
s	spatial variable for frictional energy integration
t	horizontal coordinate centred at the contact edge
t_{cycle}	time variable
$\hat{t}$	t/d – normalised horizontal coordinate centred at the contact edge
W	maximum frictional energy
$\hat{w}$	$t/d + i\,y/d$ – normalised complex coordinate
x	horizontal coordinate with origin at the centre of the contact
y	vertical coordinate with origin at the centre of the contact
$\hat{y}$	y/d – normalised vertical coordinate with origin at the centre of the contact
δ	slip displacement
σ_N	Muskhelishvili potential for the asymptotic form of the normal tractions
σ_T	Muskhelishvili potential for the asymptotic form of the shear tractions
ν	Poisson's ratio
θ	angular coordinate centred at the contact edge and measured from the contact interface (positive anticlockwise)
σ_o	bulk tension at the interface
σ_1	bulk tension applied to body 1
σ_2	bulk tension applied to body 2
σ_{fl}	fatigue limit
σ_{ij}	direct stress components, with $i,j = x,y,z$
τ_{ij}	shear stress components, with $i,j = x,y,z$
ξ	integration variable

where t is measured inwards from the contact edge, zoomed-in inset to Fig. 1, and the constant K_N is a geometry-dependent quantity which may be found from the solution to the whole contact problem, Fig. 1, by shifting the origin and taking the lead term in an expansion. For example, for a Hertzian contact of half width a, and having a peak pressure p_o the contact pressure is semi-elliptical in form

$$p(x) = p_o\sqrt{1-(x/a)^2}, \tag{2}$$

and the corresponding value of K_N is

$$K_N = p_o\sqrt{\frac{2}{a}}. \tag{3}$$

Suppose, for the time being, that the coefficient of friction, f, between the contacting bodies is sufficiently high to inhibit all slip. It follows that, at the edge of contact, the shearing traction, $q(t)$, must be square root singular, and can therefore be represented in the form

$$q(t) = \frac{K_T}{\sqrt{t}}. \tag{4}$$

The calibration for the multiplicative constant does not, here, depend on the contact geometry. If the half-width is a the application of a shearing force, Q, generates a shearing traction, $q(x)$, of the form

$$q(x) = \frac{Q}{\pi\sqrt{a^2-x^2}}, \tag{5}$$

and hence, at the trailing edge of the contact

$$K_T^Q = \frac{Q}{\pi\sqrt{2a}}. \tag{6}$$

If, instead, each body is subject to a bulk tension acting parallel with the free surface, and the difference between the tensions, $\sigma_o = \sigma_2 - \sigma_1$, the integral equation ensuring that the surface strains are matched within the contact is

$$\int_{-a}^{a}\frac{q(\xi)d\xi}{x-\xi} = \frac{\pi\sigma_o}{4}, \tag{7}$$

and this is readily inverted to give

$$q(x) = \frac{\sigma_o x}{4\sqrt{a^2-x^2}}, \tag{8}$$

so that

$$K_T^\sigma = \frac{\sigma_o}{4}\sqrt{\frac{a}{2}}. \tag{9}$$

Again, this result is independent of the profile of the contact. A comment on the sign of these quantities is appropriate: at the trailing edge the shearing force acts to the right in body 1 – both it and a dominant tension in body 2 produce a positive contribution to K_T. At the leading edge the same shearing force produces a negative contribution to K_T whilst the tension still produces a positive contribution. Very close to the ends of the contact, both forms of loading – a shear force and a difference in bulk tension – excite

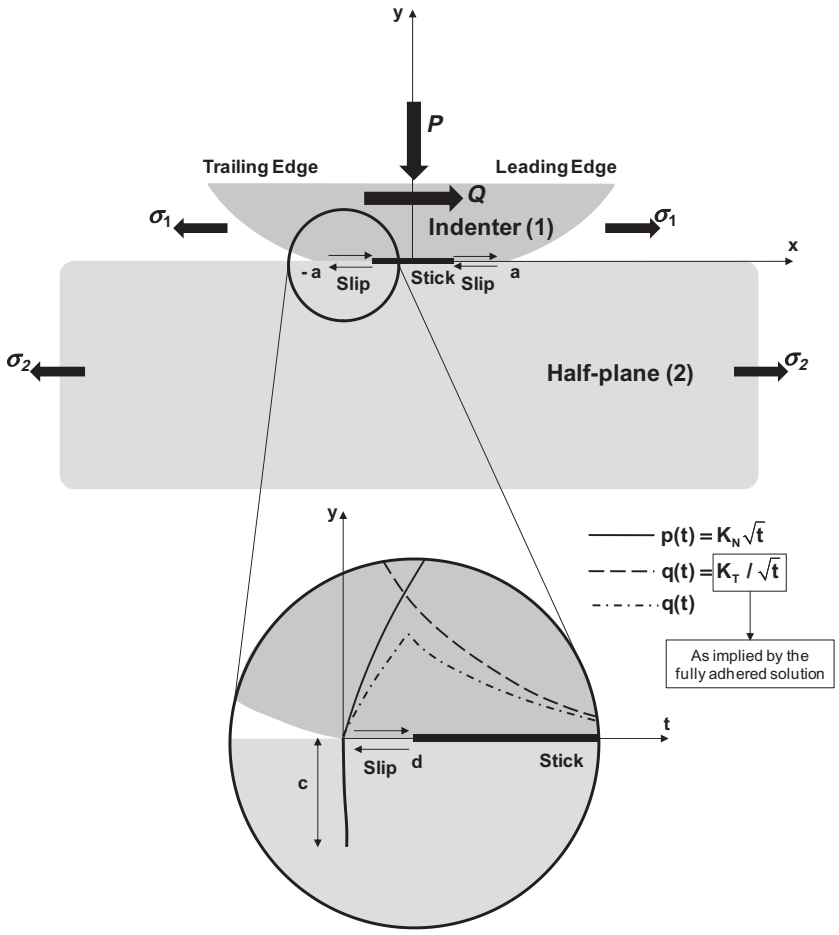

Fig. 1. Schematic of the fretting fatigue related contact problem and asymptotic characterisation (zoomed-in view of the trailing edge of the contact).

the same response in terms of the local traction distribution and therefore, over a length scale within which the tractions are appropriately represented by these asymptotic forms, so are the complete stress fields.

3. Effect of finite friction

We now relax the requirement that the coefficient of fiction be infinitely large, so that a small region of slip develops at the contact edge. Providing that the coefficient of friction is not too small, or, more exactly, the following inequality is satisfied:

$$\frac{K_T}{fK_N} \ll a, \tag{10}$$

which ensures that the slip zone is very small compared with the overall size of the contact, the asymptotic representations of the tractions remain valid, and the slip zone size, d, is given by [10]:

$$\frac{K_T}{fK_N} = \frac{d}{2}, \tag{11}$$

whilst the shearing traction, $q(t)$, is now

$$\frac{q(t)}{\sqrt{fK_N K_T}} = 2[\sqrt{\hat{t}} - \sqrt{\hat{t}-1}], \tag{12}$$

where $\hat{t} = t/d$, and this shear traction distribution is also included in the zoomed-in view of the trailing edge in Fig. 1, shown by the chain line.

4. Process zone size

We define the "process zone" as the region in which non-linear behaviour occurs, leading to plastic exhaustion, material damage and, eventually, the nucleation of a crack. Precise details of the irreversibilities are unknown and, at this scale, there is likely to be significant localisation of stress by anisotropy of the grains. As a first approximation, we take the process zone to be simply the region in which a classical bulk yield criterion is violated. It will clearly be helpful to quantify the range of loads where the process zone falls well within the slip region, and when it envelops it. To this end, we note that we already have the Muskhelishvili potentials for the problem. The contact pressure gives rise to a stress field whose Muskhelishvili potential is

$$\Phi_N(\hat{w}) = \frac{K_N\sqrt{d}}{2}\sqrt{\hat{w}}, \tag{13}$$

where $\hat{w} = (t/d + iy/d)$. We turn, now, to the shear traction, and note that, for a shearing traction distribution given by equation [12], the Muskhelishvili potential is given by

$$\Phi_T(\hat{w}) = i \times \sqrt{fK_N K_T}[\sqrt{\hat{w}} - \sqrt{\hat{w}-1}]. \tag{14}$$

Using these definitions, we can develop an expression for the state of stress in the following form:

$$\sigma_{ij}(\hat{t},\hat{y}) = K_N\sqrt{\hat{r}}g_{ij}(\theta) + \sqrt{fK_N K_T}h_{ij}(\hat{t},\hat{y}), \tag{15}$$

where $g_{ij}(\theta)$, $h_{ij}(\hat{t},\hat{y})$ are found from the Muskhelishvili potentials and $\hat{r}^2 = \hat{t}^2 + \hat{y}^2$. We may write this in a dimensionless form as

$$\frac{\sigma_{ij}(\hat{t},\hat{y})}{K_N\sqrt{d}} = \sqrt{\hat{r}}g_{ij}(\theta) + \frac{f}{\sqrt{2}}h_{ij}(\hat{t},\hat{y}). \tag{16}$$

It would clearly be possible to re-write the normalising magnitude $K_N\sqrt{d}$ in any number of different ways by using the identity for d. The second deviatoric invariant for a plane problem may be written down as

$$J_2 = \sigma_{xx}^2 + \sigma_{yy}^2 + \sigma_{zz}^2 - (\sigma_{xx}\sigma_{yy} + \sigma_{yy}\sigma_{zz} + \sigma_{zz}\sigma_{xx}) + 3\tau_{xy}^2, \tag{17}$$

and, with this scaling, von Mises' yield condition arises when

$$3k^2 = J_2, \tag{18}$$

where k is the yield stress in pure shear. We will assume that a state of plane strain exists and that Poisson's ratio is 0.3. Level lines of the normalised deviatoric invariant $\sqrt{J_2}/K_N\sqrt{d}$ may easily be found in the $(\hat{t},\hat{y})$ plane, and the only independent parameter is the coefficient of friction, f. Fig. 2 gives contours of $\sqrt{J_2}/K_N\sqrt{d}$ for two coefficients of friction, $f = 0.7,0.4$. One particular noteworthy result is that the normalised deviatoric invariant (and therefore the yield parameter) at the surface is very nearly constant across the slip region, as shown in more detail in Fig. 3, for a sensible range of coefficients of friction. By replacing $\sqrt{J_2}$ by $\sqrt{3}k$ and inverting, these contours represent an estimate of the location of the plastic front, for particular values of $K_N\sqrt{d}/k$, again for various values of the coefficient of friction. Note that we expect the severest state of stress to lie at the contact (trailing) edge only if the coefficient of friction exceeds a certain critical value. For a Hertzian contact this is about 0.26. In most fretting fatigue experiments, although the initial coefficient of friction may be relatively low, at about this threshold value, it invariably quickly rises and is usually about 0.5–0.7 (at any rate well above the value where the severest state of stress migrates to the surface), in the steady state.

This means that the value of the load at which the contact starts to go plastic (elastic limit) is only very slightly less than that at which the whole slip region yields (at least for moderate and large values of the coefficient of friction) as shown in Fig. 4; it follows that, if the load is sufficiently severe to cause local yielding the plastic region almost certainly envelops the slipping region, and the contact edge experiences a strain field controlled by a square root singular mode *II* asymptote, and hence be quite similar to a mode *II* loaded crack in nature. The same figure includes 'spots' which show where various sets of experiments conducted lie with respect to the yielding condition, and these will be discussed in detail in Section 5.

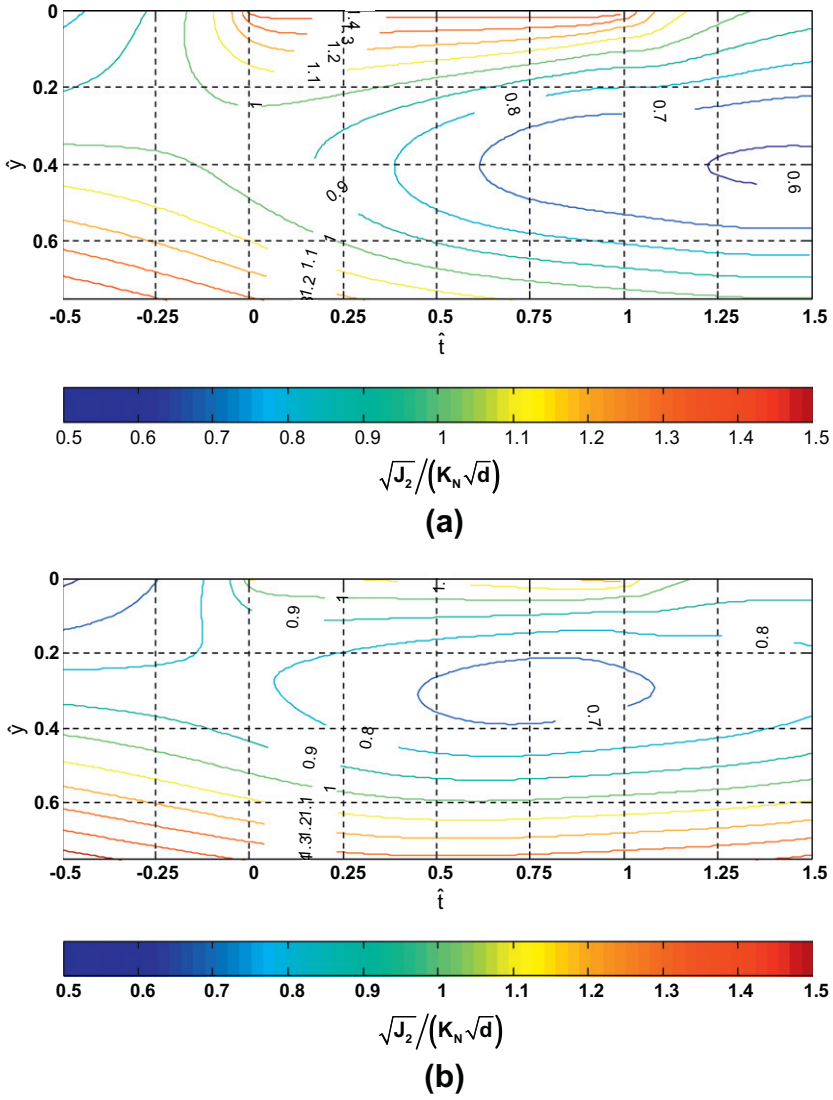

Fig. 2. Contours of the normalised deviatoric invariant, $\sqrt{J_2}/K_N\sqrt{d}$, for two coefficients of friction: (a) $f = 0.7$; (b) $f = 0.4$.

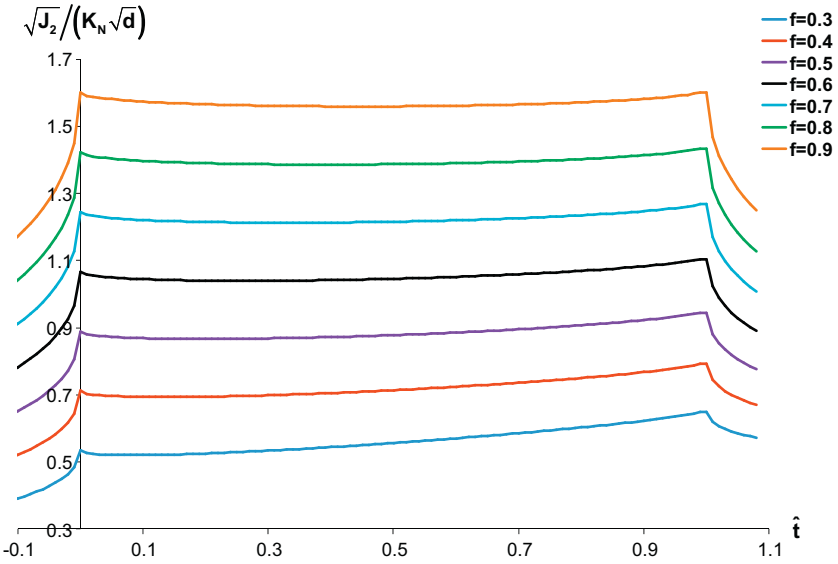

Fig. 3. Normalised deviatoric invariant, $\sqrt{J_2}/K_N\sqrt{d}$, at the contact surface for a range of coefficients of friction.

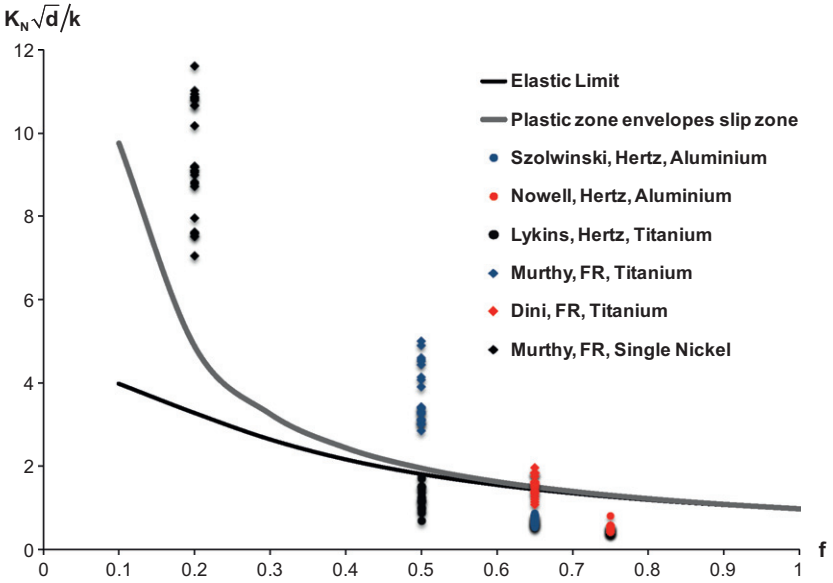

Fig. 4. $K_N\sqrt{d}/k$ vs. f map showing the elastic limit and the threshold at which the whole slip region yields. Data points represent the experimental tests in Refs. [7,9,13–18].

Turning to the fitting of the asymptotic (near-edge) solution described to particular example geometries, we require to scale the generalised stress intensity factors. For the shear traction this is geometry independent, and is given by

$$\frac{K_T^Q}{k} = \frac{Q}{2ak}\frac{\sqrt{2a}}{\pi} + \frac{\sigma_o}{k}\sqrt{\frac{a}{32}}, \tag{19}$$

and, for the particular case of a Hertzian contact, the calibration for the contact pressure solution is given by

$$\frac{K_N}{k} = \frac{p_o}{k}\sqrt{\frac{2}{a}} = \frac{P}{\pi ak}\sqrt{\frac{8}{a}}, \tag{20}$$

and these were employed in determining the locations of the 'spots' included in Fig. 4, together with a calibration for a 'flat and rounded edge contact' (denoted FR in the figure), which is rather more complicated in form and described in Appendix A. We now set out the three candidate quantities for correlating fatigue crack nucleation under incomplete contacts, but before doing so we will list the sources of the experimental data used.

5. Experimental data

The correlations to be presented have used most of the known publicly available experimental results for fretting fatigue strength. We are particularly grateful to our colleagues – Prof Farris, Dr. Murthy, Dr. Szolwinski – who were at the time, working at the University of Purdue, for making available to us the data they have published on the fretting fatigue strength of an aluminium and titanium alloy, viz., [13–15], and single crystals of nickel [16]. This supplements data from our own laboratory on aluminium alloy HE15TF found by Nowell [7] and Titanium–6Al–4V [9], and some data obtained by the US Air Force Research Laboratory at Wright Patterson [17,18]. Although many data sets are obtained using the classical Hertzian configuration, part of the database

Table 1
Material properties obtained from Refs. [7,9,13–20] for the analysed database of fretting fatigue experiments.

Material	Young's modulus E (GPa)	Poisson's ratio, ν	ΔK_{th} (MPa $\sqrt{m}$)	σ_{fl} (MPa)	k (MPa)	f	Refs.
Al alloys	74	0.3	2.1	124	270	0.65–0.75	[7,13]
Ti6Al4V	115	0.3	4.5	500	550–650	0.5–0.65	[9,14,15,17,18]
Nickel	200	0.31	7.9	450–500	600	0.2	[16,19,20]

comprises data from experiments performed using 'flat and rounded' pads, and the calibration for K_N for this geometry is given in Appendix A (as stated). The independently measured material properties – stiffness, plain fatigue strength and thresholds – assumed for these materials and used in the subsequent analysis are reported in Table 1 [7,9,13–16,18–20], where ΔK_{th} is the threshold stress intensity factor and σ_{fl} is the fatigue limit.

Fig. 4 displays the normalised magnitude of the load employed in the sets of tests just cited. The plot includes two contours derived from the calculation described earlier to find the load at the onset of plasticity – the elastic limit, and also the load at which the plastic region envelops the slip zone. We remind the reader that the difference between these loads is significant only at small values of the coefficient of friction. One of the features of the tests which surprised us is that, in many cases, the loads employed were relatively high. In particular, many of Murthy's tests were conducted at loads well above those where some plasticity might be anticipated, and any process zone involved in these experiments is likely to be large. We have therefore not included Murthy's results (and some other highly loaded cases) in our subsequent analysis, as it would not be reasonable to expect that a solution procedure which hinges on the process zone being small compared with the domain of validity of the asymptote, itself a small fraction of the contact width, to display the sequence of nesting required in these cases.

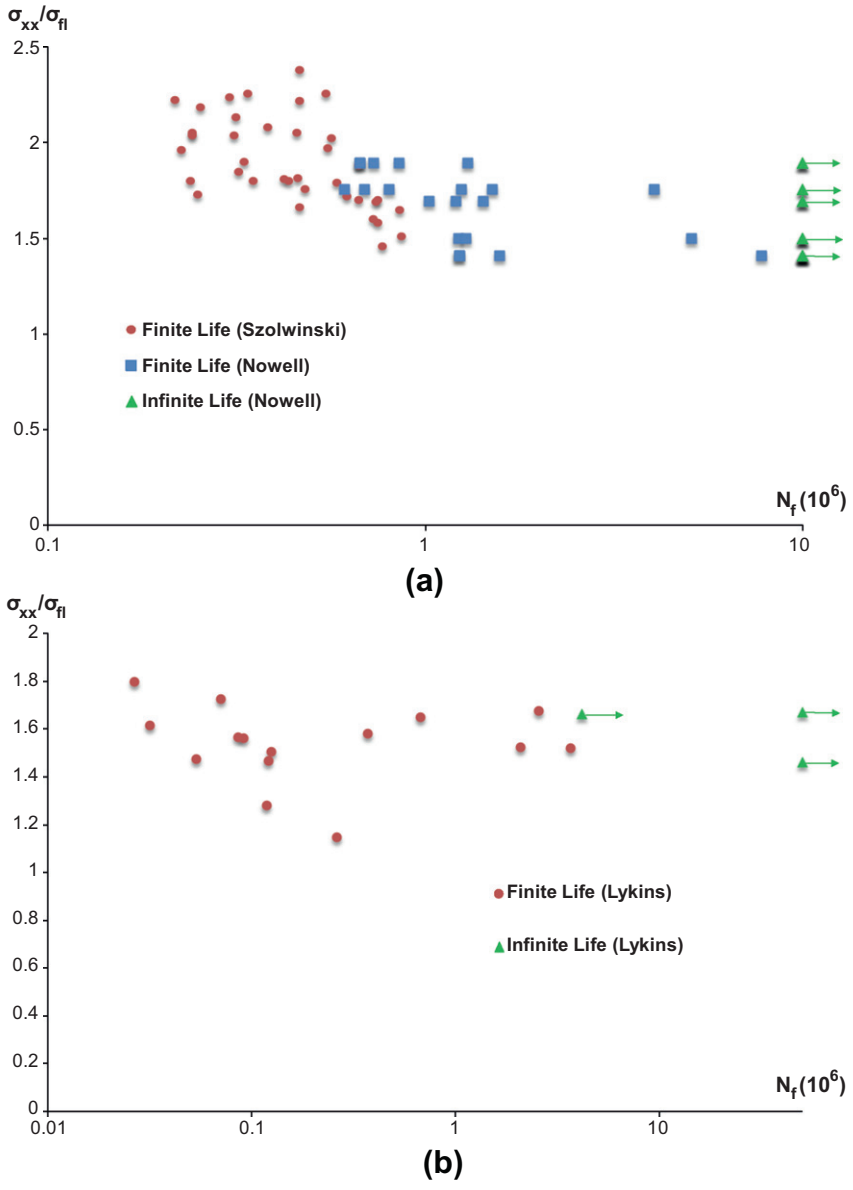

Fig. 5. *S–N* approach for the experimental results from (a) Nowell [7] and Szolwinski and [13]; (b) Lykins [18]; (c) Dini [9].

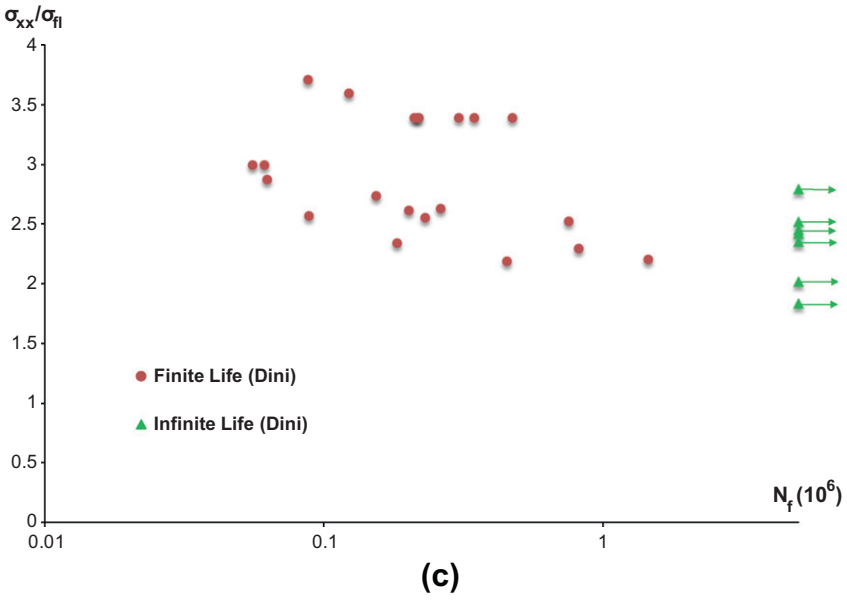

Fig. 5 (*continued*)

We now describe three possible quantities each of which may be a candidate for controlling the nucleation of fretting fatigue cracks.

6. Classical stress-controlled fatigue

The simplest way to portray fatigue data is using the classical '*S–N*' approach first developed by Wöhler about 130 years ago. This works well in plain fatigue and has been successfully applied as a design tool in its original form by many engineers to solve problems characterised by weak or no size effects and in the absence of large stress gradients. Here, we interpret '*S*' as the stress at the trailing edge of the contact, and, within the context of the asymptote, note that $\sigma_{xx}(0,0) = \sqrt{2fK_NK_T}$. Fig. 5 shows plots of the fatigue life correlated in this way. Not surprisingly, there is a very considerable spread of results, because all size information is absent from this analysis, and this is known to be of great importance. A more detailed commentary on the quality of correlation will be provided later.

One simple way of using essentially the same information, but incorporating a simple length scale *derived not from the experiment but principally from intrinsic material properties*, is to use the 'go-no-go' criterion for crack nucleation developed by Kitagawa and Takahashi (K–T) [21], which provides a means of predicting whether a very short crack will develop and eventually propagate (see Fig. 6, red[1] curve). The original paper should be consulted for details, but the essential idea is that nucleation is assumed to end, and long crack propagation starts, when the embryonic 'crack' reaches a critical length, a_0, and, therefore, short crack arrest takes place if the ΔK_I trajectory as a function of the crack length falls below the threshold (see shaded area in Fig. 6). It has been applied to fretting fatigue problems by Nowell and others [22–24], but principally in the context of a Cattaneo–Mindlin contacts. The first step in implementing within the asymptote is to determine the crack-tip stress intensity factor for a crack, of depth c, normal to the surface, and which we will assume forms at the contact edge, Fig. 1. Most cracks are observed to start either precisely at the edge of the contact, or slightly within the slip zone. Also, cracks may start in 'Stage I' (as Forsyth called it), and therefore be angled [25], but, in order to reduce the number of independent variables, we will assume that the crack grows normal to the free surface. The crack tip stress intensity factor may readily be found using the distributed dislocation method [26,27]. Note that, instead of using a description of the stress field appropriate to finite contacts, we shall assume that the critical distance is comparable with the slip region length ($d \sim a_0$), and so the surface tractions driving nucleation are adequately described by the asymptotic form. This restricts the cases which may be covered but, at the same time, it also means that the results obtained may then be applied to *any* incomplete contact. It also means that the solution is dependent on the coefficient of friction, f, and the ratio c/d only. Typical results of the trajectories describing the evolution of $\Delta K_I/\sqrt{K_NK_Td}$ with the normalised crack length are displayed in Fig. 6 (black curves).[2] We are now in a

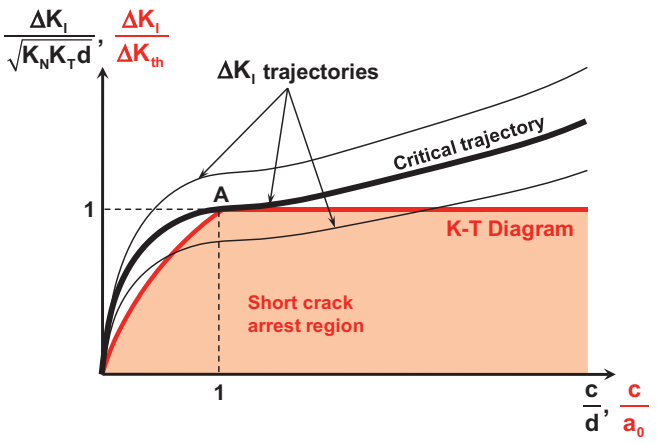

Fig. 6. Schematic of the K–T diagram and description of the normalised ΔK_I trajectories as a function of the normalised crack length.

[1] For interpretation of colour in Figs. 2–10, the reader is referred to the web version of this article.

[2] Note that here K_T corresponds to the equivalent stress intensity in shear calculated at the end of the loading cycle, and therefore, $\Delta K_T = 2K_T$ for a fully reversing loading cycle $\left(R = \frac{K_T^{min}}{K_T^{max}} = -1\right)$. Things would be different if the load ratio were greater than $R = -1$ and an extra dependent variable would need to be considered to account for the lack of symmetry of the loading history. However, detailed calculations show that there is only a weak dependence on the evolution of the threshold trajectories with R.

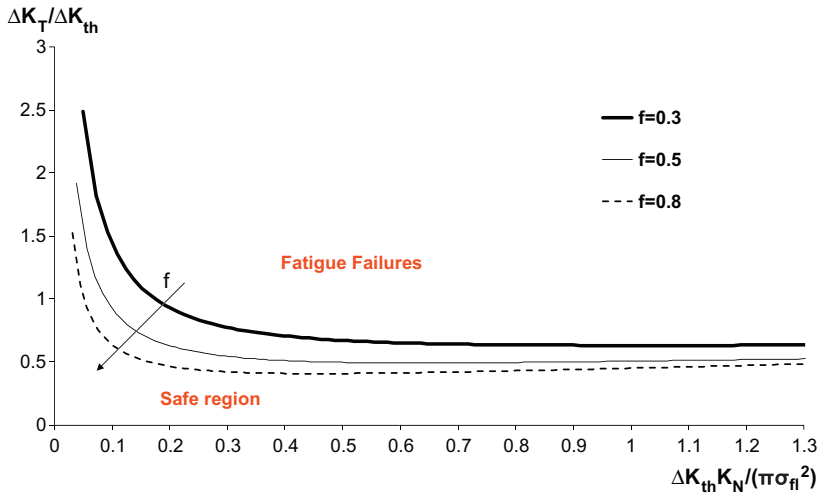

Fig. 7. Fretting fatigue threshold implied by the application of the K–T procedure using the asymptotic description for three example values of coefficient of friction, $f = 0.3, 0.5, 0.8$.

position to determine the boundary between long crack propagation and short crack arrest (which we deem to be safe in terms of design against fatigue failures). In the K–T procedure, the critical length a_o is the point at which the threshold stress intensity, ΔK_{th}, is achieved when the driving stress is given by the fatigue limit, σ_{fl}, i.e.

$$\Delta K_{th} = \sigma_{fl}\sqrt{\pi a_o}. \tag{21}$$

Looking at the critical trajectory in Fig. 6, the boundary between long crack propagation and crack self-arrest is achieved when the trajectory passes through point A. We therefore set $\Delta K_I = \Delta K_{th}$, and $c = a_o$ and, after some manipulation, we obtain the fatigue threshold implied by the application of the K–T procedure using the asymptotic description. This is shown in Fig. 7 for different values of the coefficient of friction, which becomes the only variable governing the curves in $\Delta K_T/\Delta K_{th}$ vs. $\Delta K_{th}K_N/\pi\sigma_{fl}^2$ space. These are valid for *any* incomplete contact whose stress and displacement fields can be captured by the asymptotic description proposed by the authors. The thresholds have been re-plotted in Fig. 8 (a–c) using the friction values for the experimental data reported in Table 1; the graphs now include 'spots' which show the condition present in the various experiments being used; a triangle is used when the specimen did not fail and circle and squares when failure occurred before 10^6 cycles. It may be seen that the short crack growth procedure satisfactorily predicts this boundary, but this is not surprising as the same result was found for the Cattaneo–Mindlin problem for both fully reversing loads [22] and arbitrary load ratios [9]. The advantage of the current form of the solution is that Fig. 7 is completely general and may be applied to any geometry – indeed some of the experiments here employed the 'flat and rounded' type of pad, and these have been satisfactorily correlated with the Hertz case.

7. Threshold based on a mode *II* crack-tip field

The form of the results displayed above clearly shows the inadequacy of the state of stress alone as a predictor of the fretting fatigue performance. The hybrid K–T method satisfactorily gives the finite/infinite life boundary, but cannot help us to predict the component life when it is finite (unless something is assumed about finite life thresholds or they are experimentally determined). This observation was one of the principal prompts for developing the asymptotic forms, which include size (or equivalently, stress-gradient) information. Clearly, both the normal and shear tractions have an influence on the local state of stress, but the contact pressure contribution is (a) constant in time and (b) has a negligible influence at the contact edge itself. The shear traction, on the other hand, reverses in sign and has an influence even at the contact edge. The *form* of the traction distribution depends also on both f and K_N, unless the process zone is so large that it envelops the entire slip region, and we know that this is not, in some of the experiments conducted, so. It is therefore an approximation to suggest that the range of stresses experienced at the contact edge is controlled by the range of K_T, but it is worthwhile at least to consider ΔK_T as a possible correlator of fatigue lives, and we would expect this approximation to be best when the process zone is relatively large, so as to exceed the slip region in extent, although not, of course, so large that small scale yielding conditions do not apply.

In Fig. 9 a life correlation based on ΔK_T is shown, for the different materials and with all the data we have available. The characteristic curves clearly shows a lot less spread than using the stress range, and the runout condition is also properly portrayed. It will be recalled that our original definition of K_T was for an *adhered* contact, so that the contact edge displays an implied square root singularity in stress. This is, of course, of the same order as the crack tip stress field, and with a similar local field. It follows that the stress field at the contact edge, at any rate under conditions of near adhesion, are very similar to those at the tip of a crack subjected to mode *II* loading. It further follows that the threshold for growth of a mode *II* crack might actually apply to nucleation conditions at the contact edge, and we now explore this. With this in mind, in Fig. 9 we have also included a line showing the mode *II* crack threshold, estimated as $\Delta K_{II}^{th} = 0.8 \times \Delta K_I^{th}$ (see e.g. [28,29]); this value is obviously not universal but helps providing a direct comparison between the threshold identified using ΔK_T as a correlator for fretting fatigue lives and more conventional mode *II* crack thresholds for plain fatigue. The aim of this comparison is to check if ΔK_I^{th} can be used as a threshold for ΔK_T; being able to do so would enable design against fretting to be obtained using only plain fatigue data. One of the difficulties we have had in carrying out these correlations is in ensuring that the basic materials data we have used is correct – in many cases we could not find, in the open literature, the precise values we needed for a particular material. One of the biggest problems is in obtaining a threshold (plain) fatigue crack stress intensity which has been measured at the same R-ratio as that present in the fretting test. For example, the experimental results reported in Dini [9] have been performed using an initial tensile bulk stress that offsets

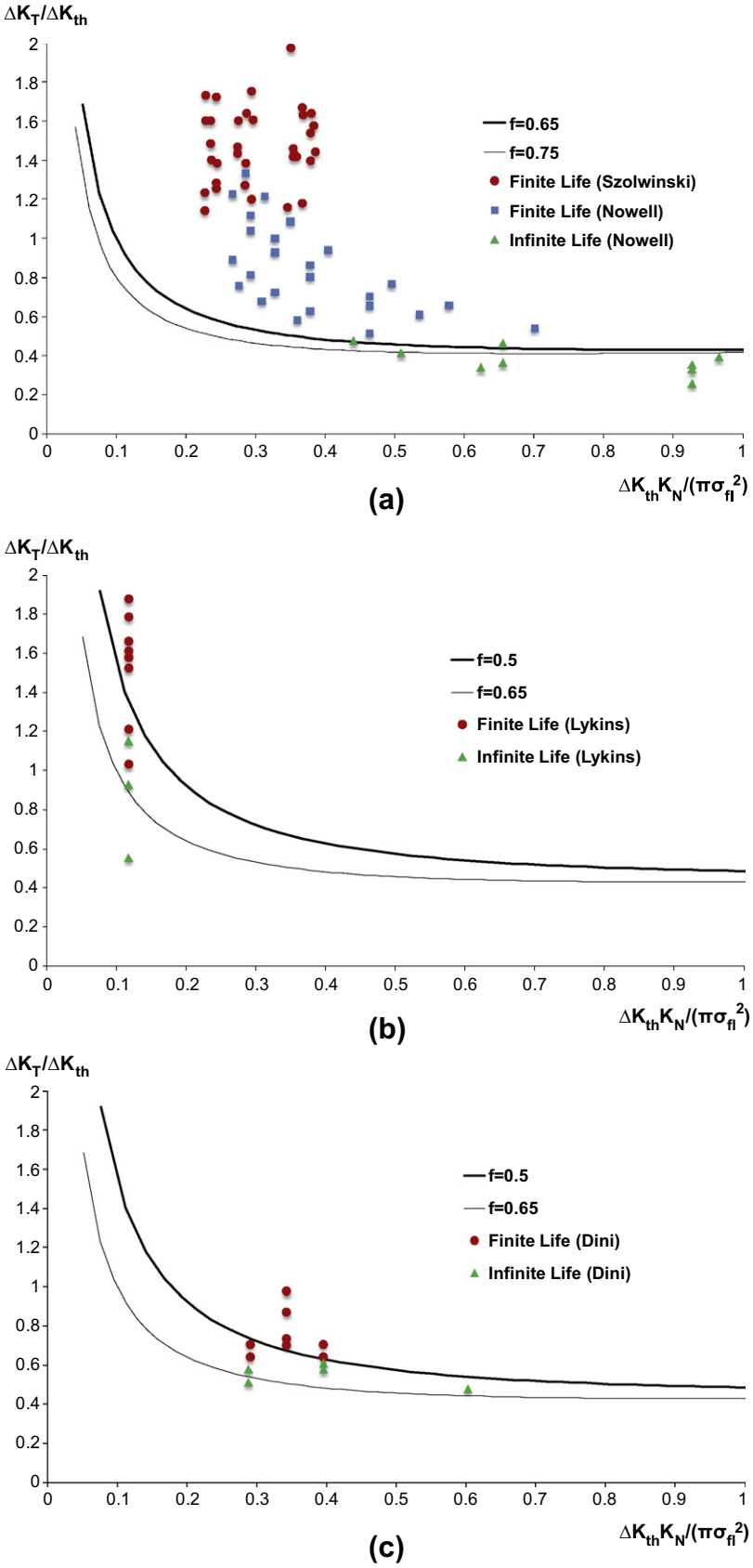

Fig. 8. Fretting fatigue thresholds implied by the application of the K–T for (a) the aluminium alloys used in Refs. [7,13] and the friction coefficients measured by Szolwinski and Nowell; (b) and (c) Ti6Al4V and the friction coefficients measured by Lykins [18] and Dini [9]. Data points represent the experimental tests performed in (a) Refs. [7,13]; (b) Ref. [18]; (c) Ref. [9].

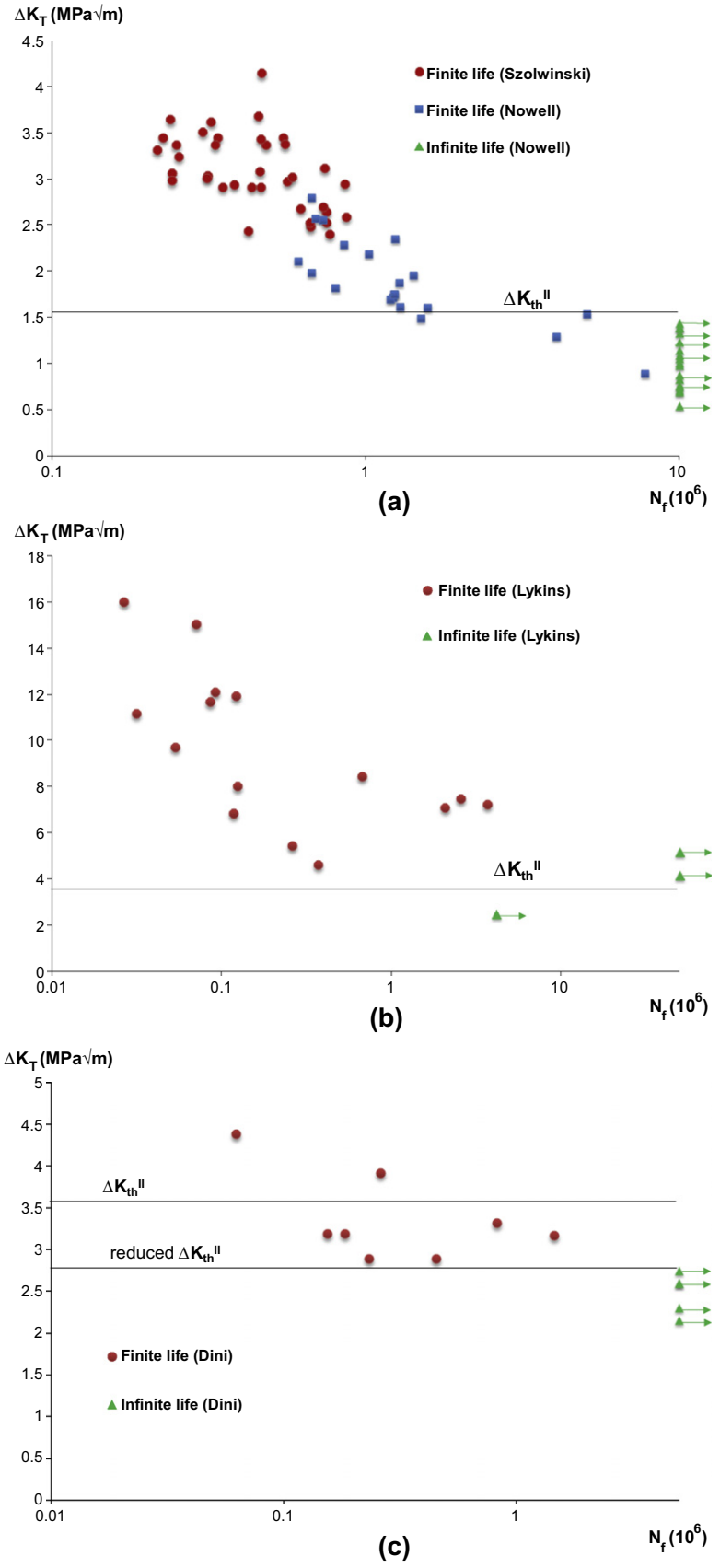

Fig. 9. Life correlation based on ΔK_T for the tests reported in (a) Refs. [7,13]; (b) Ref. [18]; (c) Ref. [9].

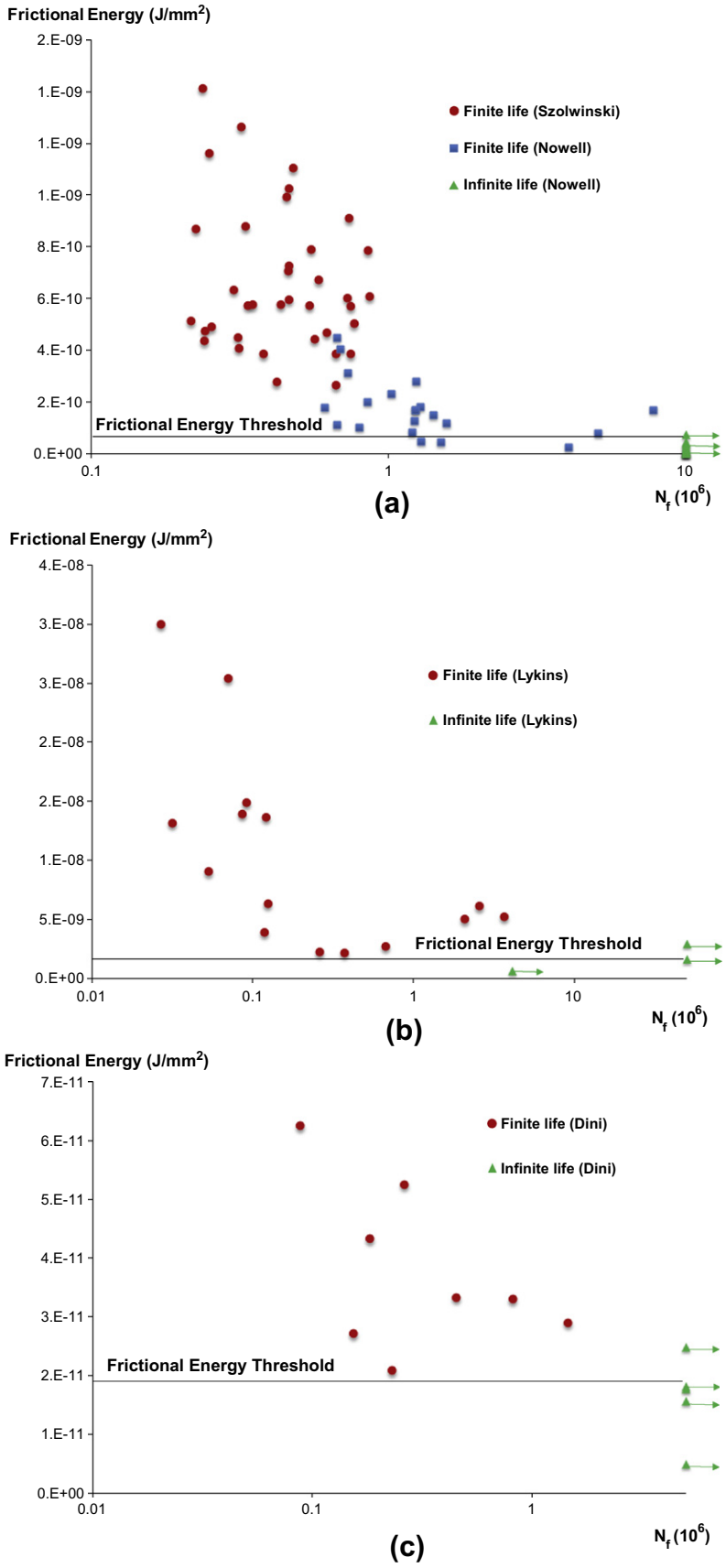

Fig. 10. Life correlation based on frictional energy expenditure for the tests reported in (a) Refs. [7,13]; (b) Ref. [18]; (c) Ref. [9].

the equivalent load ratio to $R = 0.5$–0.6. The R ratio at which the threshold was measured quoted in the table was -1, and this suggests that a reduced ΔK_{II}^{th} should be applied to Dini's results. This is displayed in Fig. 9c as a 'reduced ΔK_{th}^{II}', and illustrates the difficulty in carrying out these correlations with an incomplete set of data.

8. Frictional energy expenditure density

The principal objection to the above correlation is that the influence of both f and K_N were ignored: of course, in the experiments the contact pressure, and hence K_N were kept constant, so that they relate to a static stress field, and hence one which does not, in itself, produce damage, because it should be recalled that the asymptote was developed under conditions of, as a first estimate, full adhesion (and this is a necessary step so that the effects of a shearing force and bulk tension can be consistently treated), so that the coefficient of friction might be regarded as a further controlling parameter, *unless* the process zone bridged the slip region.[3] An alternative quantity which might sensibly be used to correlate nucleation life is the magnitude of the density of irreversible frictional energy expended within the slip region. Note that this is a pointwise quantity and has a maximum value towards the centre of the slip region [30]. For a monotonically increasing shearing force (and hence K_T), the maximum frictional energy expended per unit area at the steady-state can be expressed as:

$$W = C\frac{K_T^{\max 2}}{K_N\sqrt{d}} = C\frac{K_T^{\max 2}}{K_N}\sqrt{\frac{2K_T}{fK_N}} = C'\frac{K_T^{\max 5/2}}{fK_N^{3/2}}, \tag{22}$$

where C' can be found by performing the following integration as described in [30]: $W = \int_{cycle} q(s,t_{cycle})d\delta(s,t_{cycle})$, where δ is the slip displacement at every point in space, s, and time, t_{cycle}, during the loading cycle. Analytical (as done for an example case in [30]) or numerical integration can also be performed to obtain the evolution of the slip displacements during the entire cycle for different loading scenarios. This allows closed form analytical or equivalent numerical solutions to be determined for all experimental cases; we have therefore extended the range of the previous solution, and now give the calibration constant, C', for all conditions. A plot of correlated lives using this quantity is shown in Fig. 10.

The results of this correlation differ in character from those earlier, because in each of the other possible criteria there is, existing, some threshold information obtained by independent experiment – σ_{fl} for the S–N curve, σ_{fl} and ΔK_{th} for the K–T procedure, and ΔK_{th} alone for the 'mode II crack' method – whereas here we have no pre-existing materials data available. We are therefore free to choose the threshold condition for infinite life, and have inserted what seems to be the best choice in Fig. 10a for the aluminium alloy, (b) for the titanium alloy cylindrical pads and (c) for the titanium alloy flat and rounded ends pads. This correlation has met with mixed success; in each case, the tests are correctly ranked with little spread and few outliers; and, the cut-off threshold is very distinct. What is difficult to explain is why the two sets of results for the titanium tests do not compare better with each other. The whole thesis of using an asymptotic form to capture the threshold condition is that such form should be capable of collocation into a wide range of possible geometries, and it is disappointing that the two sets of tests on titanium apparently give markedly differing thresholds. One possible explanation for this could be that the length scale inherent in the asymptote does not, here, figure in the final quantity being employed, viz. the maximum frictional energy expenditure per unit area, which arises only at a spot. All information concerning size effects is, in this sense, lost again here; however, if the calculation is extended to find the total frictional energy dissipated per loading cycle (which contains information about the extent of slip and therefore includes the asymptotic length scale), the results show the same trends seen in Fig. 10 but not included here. It is argued that, although larger values of energy dissipation at the contact interface might help promote crack nucleation [31], the frictional energy expenditure is in reality more directly linked to the tendency of the surfaces to wear [32] rather than to initiation of the fatigue process. This in turn seems to be controlled (at least in the cases analysed here, which are characterised by very low wear) by the stress and strain fields in the proximity of the contact edge, which the asymptotic description correctly captures, as shown in the previous sections. It is envisaged that the frictional energy dissipation density will indeed provide a good correlator for fretting wear tests as already suggested by others working in the field (see e.g. [32]). The use of the asymptotic approach proposed by the authors provides a rapid tool to characterise this in closed form and its potential application to fretting wear tests will be explored in future contributions.

9. Discussion and conclusions

This paper has considered in detail the nature of the contact edge stress field for incomplete contacts capable of description by half-plane theory, and how it might affect crack nucleation life under fretting conditions. We have taken as our starting point the work on asymptotic representations of the local field already discovered, and added further properties relevant to the nucleation process. These results have been used to form four potential correlators of fretting fatigue crack nucleation lives: the first is the obvious one of stress range at the critical point. This is the most obvious choice based on classical S–N (Wöhler) principles. It is clearly poor, because all size effect information is neglected. The K–T approach to determining the threshold for crack nucleation, and which bridges classical fatigue and fracture mechanics principles was also used, and this was shown satisfactorily to predict the boundary between finite and infinite life. This results is a generalisation of that already found for a Hertz contact, and provides, in the form displayed in Fig. 7, a usable design tool for the avoidance of fretting failures.

Two further correlators of nucleation lives were then introduced, based solely on the multipliers of the asymptotic solutions: the first is simply an approximate correlation of the reversing stress field due to shear loading, and seems very satisfactorily to collapse the experimental data; it also captures size information inherent in the experimental contact very well. The second is based on the quantity controlling nucleation being the maximum density of irreversible frictional energy expenditure.

It is worth emphasising that the procedures described involve no 'fitting parameters' or volume averages. In all cases the possible controlling variable correlates at least reasonably well with the number of cycles to failure, and provides some kind of trend, of varying quality. In the case of all but the energy correlation, there is also *some* pre-existing materials data with which the quantity may be compared – and obtained from plain fatigue theory. This prompts the obvious question 'Does fretting exacerbate or ameliorate nucleation conditions compared with a plain problem?' Prima facie, it would seem that both the K–T and ΔK_T methods suggest that the effect is quite neutral. This might be due to the fact that most of the experimental results collated and used in the present contribution were designed to study partial slip fretting configurations where only a very limited amount of wear takes place and the fatigue phenomenon is almost entirely controlled by the stress concentration and the stress and strain gradients at the contact

[3] Note that a process zone in a monolitic material and an equivalent zone bridging a slipping interface differ in that in the latter there is a line (the interface) along which frictional as well as plastic slip may occur.

edges [33]; it also explains the partial success that conventional multiaxial fatigue approaches have met in predicting fretting lives in most of the work carried out by different groups around the world (see e.g. [34,16,35]). A further characteristic of the asymptotic correlators used here is that, whereas the asymptotes used in the K–T and ΔK_T methods incorporate stress gradient or size information (particularly in the latter approach), they do not function in this way in the energy density approach. It should be also highlighted that since the accumulated frictional energy dissipated at the contact interface plays a fundamental role in assessing fretting wear damage, the closed form solutions developed by the authors can be easily implemented to study the interplay between wear and fatigue damage and, therefore, can be used to develop predictive tools for scenarios where these two mechanisms cannot be decoupled and only semi-empirical parameters are available to provide estimate of damage [31,36].

Finally, it should be pointed out that the asymptotic descriptions formulated can also potentially be incorporated in numerical tools (as super-elements in FEM or BEM formulations) and/or be used for fast assessment of fretting fatigue life using conventional multiaxial criteria. Furthermore, the asymptotic formulation could also be used as the starting point to incorporate other properties relevant to the nucleation process that have been neglected in the present contribution, e.g. material microstructure and localised plasticity at individual grain level [37]. It is envisaged that by adding microstructural details [39] and considering plasticity and damage at the microscale (see e.g. [38]) would help shedding light on important issues, such as microstructural sensitivity [40] and the importance of material-inherent length scales. The first step to be performed in this direction is the direct comparison between the region of validity of the asymptotic solution an the characteristic grain sizes of the materials tested. The lack of microstructural data for the majority of the test series considered in this article does not allow this comparison to be performed; however, the systematic study of the role of microstructural features in the assessment of fretting fatigue performance within the asymptotic framework will constitute the object of future investigations.

Appendix A. Calibration for asymptote K_N for rounded edge contact

The contact pressure for a radiused semi-infinite flat and rounded punch characterised by the edge radius R, can be written as [41]:

$$p(x) = \frac{3K_N}{4\sqrt{a_{round}^3}}\left[2\sqrt{x a_{round}} + [x - a_{round}]\ln\left|\frac{\sqrt{a_{round}} - \sqrt{x}}{\sqrt{a_{round}} + \sqrt{x}}\right|\right], \qquad (23)$$

where a_{round} is the radiused portion of the contact and can be found from [42], $E^* = E/[2(1-\nu^2)]$ for elastically similar materials, and K_N can be defined as:

$$K_N = \frac{-2E^*\sqrt{a_{round}^3}}{3\pi R}. \qquad (24)$$

If $t/a_{round} \gg 1$, the pressure varies in the forum $p(t) = \frac{K_N}{\sqrt{t}}$. If the observation point is very close to the edge of the contact, $0 < t/a_{round} \ll 1$, the pressure varies in the form:

$$p(t) = \frac{3K_N\sqrt{t}}{a_{round}}. \qquad (25)$$

References

[1] O'Connor JJ, Johnson KL. The role of surface asperities in transmitting tangential forces between metal. Wear 1963;6(2):118.

[2] Khadem R, O'Connor JJ. Axial compression of an elastic circular cylinder in contact with two identical elastic half spaces. Int J Eng Sci 1969;7(8):785–800.

[3] Bramhall, Studies in fretting fatigue. DPhil Thesis, University of Oxford; 1973.

[4] O'Connor JJ. The role of elastic stress analysis in the interpretation of fretting fatigue failures. In: Waterhouse RB, editor. London: Fretting Fatigue, Applied Science; 1981.

[5] Cattaneo C. Sul conttatto di due corpi elastici: distribuzione locale degli storzi. Pend.d'Acad naz.dei Lincei, Series 6 1938;27. p. 342, 434, 474.

[6] Mindlin RD. Compliance of elastics bodies in contact. J Appl Mech (Trans ASME, Series E) 1949;16:259.

[7] Nowell D. An analysis of fretting fatigue, D.Phil Thesis, University of Oxford; 1988.

[8] Nowell D, Dini D, Hills DA. Recent developments in the understanding of fretting fatigue. Eng Fract Mech 2006;73(2):207–22.

[9] Dini D. Studies in fretting fatigue with particular application to almost complete contacts. D.Phil Thesis,University of Oxford; 2004.

[10] Dini D, Hills DA. A method based on asymptotics for the refined solution of almost complete partial slip contact problems. Eur J Mech A – Solids 2003;22(6):851–9.

[11] Dini D, Hills DA. Bounded asymptotic solutions for incomplete contacts in partial slip. Int J Solids Struct 2004;41(24–25):7049–62.

[12] Hills DA, Dini D. A new method for the quantification of nucleation of fretting fatigue cracks using asymptotic contact solutions. Tribol Int 2006;39(10):1114–22.

[13] Szolwinski MP, Farris TN. Observation, analysis and prediction of fretting fatigue in 2024-T351 aluminum alloy. Wear 1998;221(1):24–36.

[14] Murthy H, Mseis G, Farris TN. Life estimation of Ti–6Al–4 V specimens subjected to fretting fatigue and effect of surface treatments. Tribol Int 2009;42(9):1304–15.

[15] Gean MC, Farris TN. Elevated temperature fretting fatigue of Ti-17 with surface treatments. Tribol Int 2009;42(9):1340–5.

[16] Murthy H, Gao G, Farris TN. Fretting fatigue of single crystal nickel at 600 °C. Tribol Int 2006;39(10):1227–40.

[17] Lykins CD, Mall S, Jain V. An evaluation of parameters for predicting fretting fatigue crack initiation. Int J Fatigue 2000;22:703–16.

[18] Lykins CD. An investigation of fretting fatigue crack initiation behavior of the titanium alloy Ti–6Al–4 V. PhD dissertation, University of Dayton; 1999.

[19] Morrissey RJ, Golden PJ. Fatigue strength of a single crystal in the gigacycle regime. Int J Fatigue 2007;29(9–11):2079–84.

[20] Shyam A, Padula II SA, Marras SI, Milligan WW. Fatigue-crack-propagation thresholds in a nickel-base superalloy at high frequencies and temperatures. Metal Mater Trans A 2002;33 A:1949–62.

[21] Kitagawa, H. Takahashi S. Applicability of fracture mechanics to very small cracks or the cracks in the early stage. In: Proceedings of the second international conference on mechanical behavior of materials. Metals Park (OH): ASM; 1976. p. 627–31.

[22] Araujo JA, Nowell D. Analysis of pad size effects in fretting fatigue using short crack arrest methodologies. Int J Fatigue 1999;21(9):947–56.

[23] Dini D, Nowell D, Dyson IN. The use of notch and short crack approaches to fretting fatigue threshold prediction: theory and experimental validation. Tribol Int 2006;39(10):1158–65.

[24] Fouvry S, Nowell D, Kubiak K, Hills DA. Prediction of fretting crack propagation based on a short crack methodology. Eng Fract Mech 2008;75(6):1605–22.

[25] Hills DA, Nowell D. Mechanics of fretting fatigue. Dordrecht, The Netherlands: Kluwer Acadamic Publishers; 1994.

[26] Nowell D, Hills DA. Open cracks at or near free edges. J Strain Anal Eng Des 1987;22(3):177–86.

[27] Hills DA, Kelly PA, Dai DN, Korsunsky AM. Solution of crack problems: the distributed dislocation technique. Kluwer Acadamic Publishers; 1996.

[28] Otsuka A, Mori K, Mitata T. The condition of fatigue crack growth in mixed mode condition. Eng Fract Mech 1975;7:429–39.

[29] Otsuka A, Tohgo K, Matsuyama H. Fatigue crack initiation and growth under mixed mode loading in aluminum alloys 2017-T3 and 7075T6. Eng Fract Mech 1987;28(6):721–32.

[30] Dini D, Sackfield A, Hills DA. Comprehensive bounded asymptotic solutions for incomplete contacts in partial slip. J Mech Phys Solids 2005;53(2):437–54.

[31] Ruiz C, Boddington PHB, Chen KC. An investigation of fatigue and fretting in a dovetail joint. Exp Mech 1984;24(3):208–17.

[32] Fouvry S, Paulin C, Liskiewicz T. Application of an energy wear approach to quantify fretting contact durability: introduction of a wear energy capacity concept. Tribol Int 2007;40(10–12):1428–40.

[33] Nowell D, Dini D. Stress gradient effects in fretting fatigue. Tribol Int 2003;36(2):71–8.

[34] Araujo JA, Nowell D. The effect of rapidly varying contact stress fields on fretting fatigue. Int J Fatigue 2002;24(7):763–75.

[35] Navarro C, Munoz S, Dominguez J. On the use of multiaxial fatigue criteria for fretting fatigue life assessment. Int J Fatigue 2008;30(1):32–44.

[36] Ding J, Houghton D, Williams EJ, Leen SB. Simple parameters to predict effect of surface damage on fretting fatigue. Int J Fatigue 2011;33(3):332–42.

[37] Korsunsky AM, Dini D, Dunne FPE, Walsh MJ. Comparative assessment of dissipated energy and other fatigue criteria. Int J Fatigue 2007;29(9–11):1990–5.

[38] Goh C-H, McDowell DL, Neu RW. Plasticity in polycrystalline fretting fatigue contacts. J Mech Phys Solids 2006;54:340–67.
[39] Weinzapfel N, Sadeghi F, Bakolas V. An approach for modeling material grain structure in investigations of Hertzian subsurface stresses and rolling contact fatigue. ASME J Tribol 2010;132(4):041404.
[40] Zhang M, McDowell DL, Neu RW. Microstructure sensitivity of fretting fatigue based on computational crystal plasticity. Tribol Int 2009;42(9):1286–96.
[41] Mudadu A, Hills DA, Barber JR, Sackfield A. The application of asymptotic solutions to characterising the process zone in almost complete frictional contacts. Int J Solid Struct 2003;41:385–97.
[42] Ciavarella M, Hills DA, Monno G. The influence of rounded edges on indentation by a flat punch. Proc Inst Mech Eng – Part C: J Mech Eng Sci 1998;212(4):319–27.